We are IntechOpen, the world's leading publisher of Open Access books Built by scientists, for scientists

6,900
Open access books available

185,000
International authors and editors

200M
Downloads

Our authors are among the

154
Countries delivered to

TOP 1%
most cited scientists

12.2%
Contributors from top 500 universities

WEB OF SCIENCE™

Selection of our books indexed in the Book Citation Index in Web of Science™ Core Collection (BKCI)

Interested in publishing with us?
Contact book.department@intechopen.com

Numbers displayed above are based on latest data collected.
For more information visit www.intechopen.com

Chapter 1

Earthquake Instrumentation

Jae Cheon Jung

Additional information is available at the end of the chapter

http://dx.doi.org/10.5772/66215

Abstract

Earthquake detectors (seismic instruments) are used to measure low-frequency ground motion caused by earthquakes. They detect the seismic waves created by ground motions and convert the wave motions into electronic signals, which are measurable. Two measurement principles are widely used in the industry sector to detect the strong motion of earthquake that require high sensitivity: force-balanced acceleration and servo acceleration with a feedback loop. In this chapter, the motion of the mass as a function of the ground displacement is discussed with a differential equation resulting from the equilibrium of forces. In addition, the transfer functions of both instruments are investigated by using Matlab® Simulink. This technology is applied in NPP (nuclear power plant) to ensure the safety of the plant in systems, such as the SMS (seismic monitoring system) and the ASTS (automatic seismic trip system). SMS provides monitoring and recording capability, whereas ASTS makes a decision to trip the NPP when the PGA (peak ground acceleration) exceeds the pre-defined value, which is determined based on the ground conditions.

Keywords: earthquake detector, seismic instruments, accelerometer, force balanced acceleration, servo acceleration, transfer function

1. Introduction

Earthquake detection instrumentation is widely used in many industries to secure the system, structure and components. In addition, early warning of incident seismic wave is critical to safety of human lives. On 12 September 2016, South Korea experienced the most powerful earthquake ever recorded in the country since measurements began in 1978. A 5.8-magnitude earthquake struck the historic city of Gyeongju and the people were subjected to a series of aftershocks affecting their daily lives [1]. Buildings built inside the historic district were not

INTECH
open science | open minds

© 2017 The Author(s). Licensee InTech. This chapter is distributed under the terms of the Creative Commons Attribution License (http://creativecommons.org/licenses/by/3.0), which permits unrestricted use, distribution, and reproduction in any medium, provided the original work is properly cited. CC BY

strong enough to sustain seismic incident despite its low destructive power. Luckily, since the frequency of the wave was higher than 16 Hz, a catastrophic falling down of buildings was not experienced. This tells the relationship among magnitude, wave frequency and the destructive power. Earthquake detection instrumentation has been improved to detect the magnitude and frequency effectively. Historically, the first seismic instrument was invented in Han dynasty. Modern instruments are based on electronic sensors which are able to detect tri-axial acceleration.

In order to investigate both theory and application of earthquake instruments, the mathematical expression of the instrument is defined by the motion of the mass-spring-damper system. Then the differential equation resulting from the equilibrium of forces is discussed. In addition, the transfer functions of both force balanced and servo balanced and feedback circuit are analysed. Finally, the application of earthquake instrument in the nuclear power plant is introduced.

2. Mathematical expression

Let us define a single seismic instrument having mass, spring and dashpot as shown in **Figure 1**. A dashpot is a device that provides viscous friction or damping [2]. The dashpot absorbs energy. This spring-mass-dashpot system can be expressed using Newton's second law as represented in Eq. (1):

$$\text{(D.E.) } m\ddot{y} = -ky - b\dot{y} + u \tag{1}$$

$$\text{(T.F.) } ms^2Y(s) = -kY(s) - bsY(s) + U(s) \tag{2}$$

$$G(s)\frac{Y(s)}{U(s)} = \frac{1}{ms^2 + bs + k} \tag{3}$$

The mathematical expression of the system above can be expressed as Eq. (1). The transfer function of Eq. (1) can be obtained as Eqs. (2) and (3) by taking Laplace transformation.

The motion of the mass as a function of the ground displacement is given by a differential equation resulting from the equilibrium of forces as shown in Eq. (4) [3].

$$Fs + Fr + Fg = 0 \tag{4}$$

where $Fs = -kx$ (k is the spring constant);

$Fr = -bx$ (b is the friction coefficient);

$Fg = -mu$ (m is the spring mass).

http://dx.doi.org/10.5772/66215

When the seismic instrument moves slowly, the acceleration and velocity become negligible, it records ground acceleration. If however, movement is fast enough, the acceleration of the mass dominates and the ground displacement is recorded.

Figure 2 shows the seismic instrument under ground motion. Where the u_g is the ground displacement, x_r is displacement of the seismometer mass and x_0 is the mass equilibrium position.

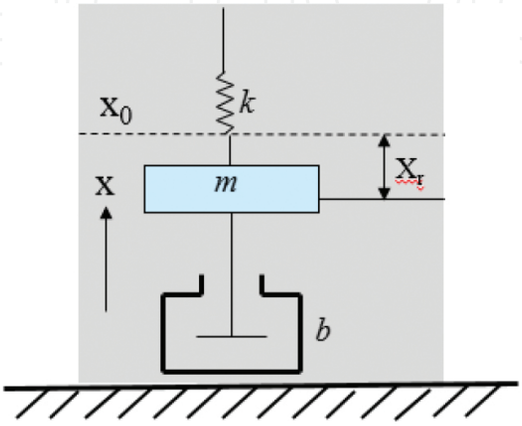

Figure 1. Spring-mass-dashpot system.

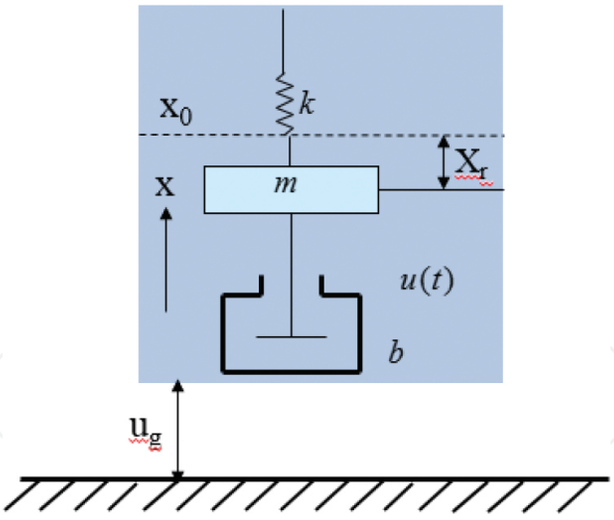

Figure 2. Concept of seismic instrument under ground motion.

In general, the frequency of the seismic wave tends to be increased if the magnitude of the wave is getting smaller. The ground motion has very low-frequency profile due to the movement of the earth.

This study is focused on the plant industry application of the earthquake instrument. In this case, the detector covers DC to 50 Hz frequency components.

3. Tri-axial accelerometer

The tri-axial accelerometer has been widely used in industrial applications. An accelerometer is a sensor which can detect the earthquake-induced motion. The tri-axial accelerometer has a coil in the sensor that is suspended to it. When the accelerometer detects the earthquake-induced motion, the coil is moved and the voltage is induced proportionally to the variation of magnetic force. This voltage is converted to acceleration.

The tri-axial accelerometer detects incident seismic waves from longitudinal (L), transverse (T) and vertical (V) direction using three identical sensors as illustrated in **Figure 3**. In general, each accelerometer has a feedback amplifier in consideration of the stability of the sensor output. Moreover, an added RC filter eliminates the high-frequency component from the output. The accelerometers are installed at free-field where the earthquake ground motion is detected by the surface motion.

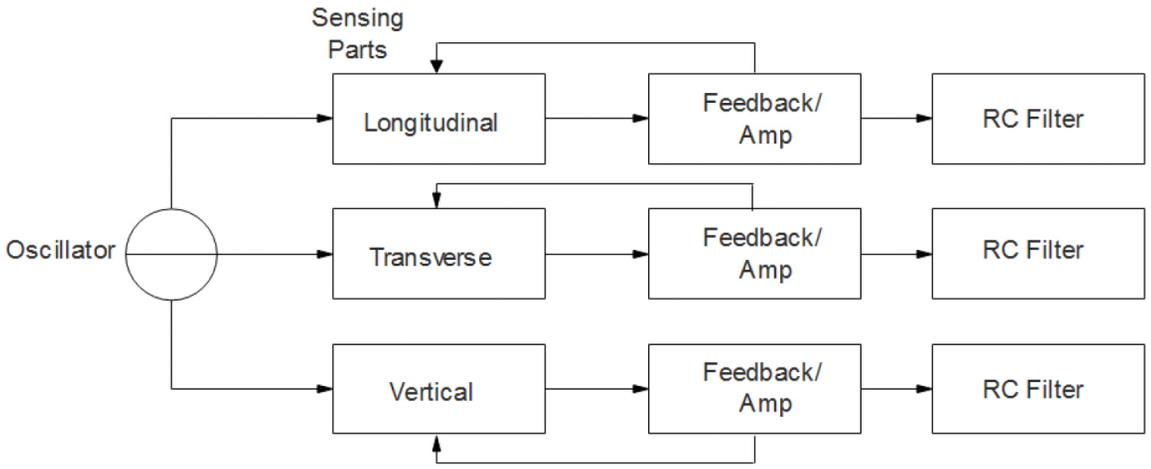

Figure 3. Concept of tri-axial accelerometer.

3.1. Types of accelerometers

An accelerometer detects low-frequency component from the earthquake ground motion. Two measurement principles are used to detect a strong motion earthquake requiring high sensitivity: open-loop type or closed-loop type with a feedback loop. In the plant industry, two sensor types have been used; force balanced acceleration using a pendulum, and servo acceleration with a feedback loop.

3.1.1. Force balanced acceleration using pendulum

In this section, the FBA-23 (by Kinemetrics Inc.) accelerometer is analysed to provide a more detailed operational theory of pendulous type servo sensors. As seen in **Figure 4**, FBA-23 consists of three-axis FBAs (force balanced accelerators) for detecting incident seismic waves in (L), (T) and (V) directions. Each accelerometer is identical, however, the vertical one has an active oscillator circuit as an additional function.

http://dx.doi.org/10.5772/66215

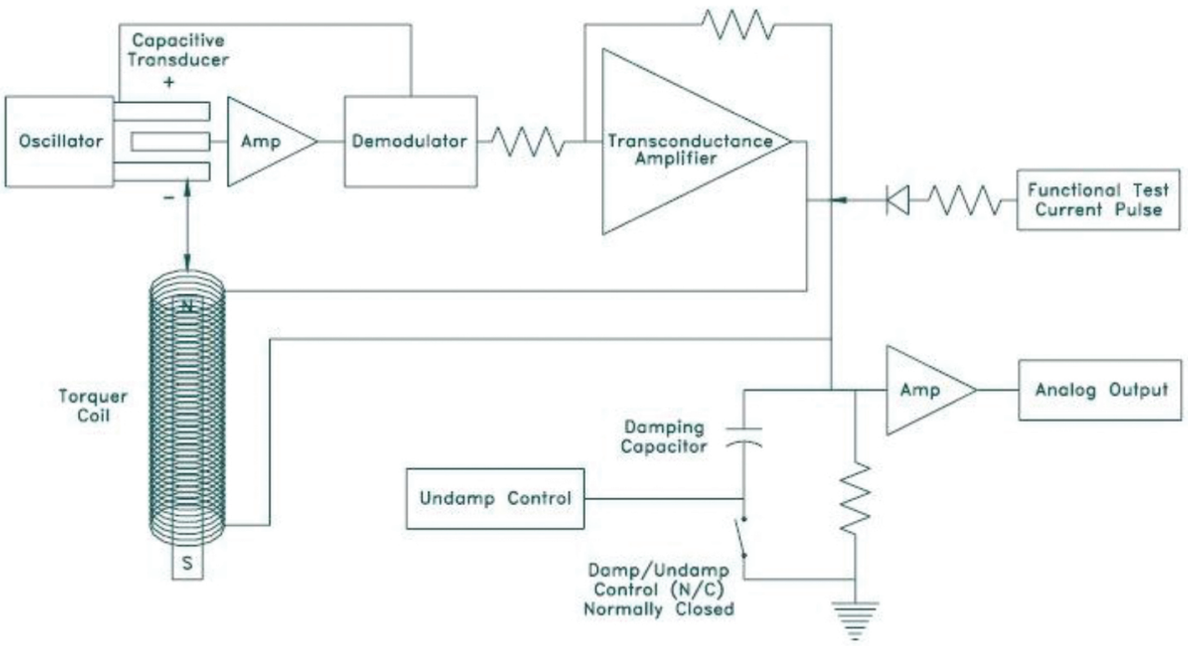

Figure 4. Simplified circuit of FBA-23 [4].

The electrical circuit of FBA-23 has a non-inverting amplifying circuit for adjusting the polarity of the output signal. The transfer function of the accelerometer can be expressed by Eq. (5).

$$\frac{E_{\mathrm{OUT}}}{E_{\mathrm{DC}}} = \frac{\omega_n^2}{s^2 + 2\zeta\omega_n s + \omega_n^2} \tag{5}$$

where ω_n = natural frequency; s = Laplacian; ζ = damping factor.

The solution of Eq. (5) can be denoted by the second order equation having two poles (p_1, p_2) as shown in Eqs. (6) and (7).

$$p_{1=} - \zeta\omega_n + \mathrm{j}\omega_n\sqrt{1-\zeta} \tag{6}$$

$$p_{2=} - \zeta\omega_n - \mathrm{j}\omega_n\sqrt{1-\zeta} \tag{7}$$

The circuit has sensitivities of 0.25, 0.5, 1, 2 and 4 g full scale. This corresponds to normal absolute sensitivity at DC.

The second order transfer function in Eq. (5) has natural frequencies of 50, 90 or 100 Hz. In addition, if we consider the damping factor of 0.707, then the two poles (p_1, p_2) are located in the left half of the s-plane. The transfer function of this accelerometer can be rewritten as Eq. (8) having two poles.

$$\frac{E_{\text{OUT}}}{E_{\text{DC}}} = \frac{\omega_n^2}{s^2 + 2\zeta\omega_n s + \omega_n^2} = \frac{\omega_n^2}{(s - P1)(s - P2)} \tag{8}$$

From Eq. (8), the natural frequency and damping factor of this instrument can be calculated as Eqs. (9) and (10) respectively.

$$\omega_n = 2 \cdot \pi \cdot 50 = 314.159 \tag{9}$$

$$\zeta = 0.2550(\text{for } 1.0 \text{ g}) \tag{10}$$

The poles are then calculated as, $P1$ = -222.1 + j222.1 rad/s and $P2$ = -222.1 - j222.1 rad/s. Therefore, the resultant transfer function of this system becomes Eq. (11)

$$TF = \frac{98696}{s^2 + 160.22s + 98696} \tag{11}$$

Figure 5 shows the Matlab Simulink results when the step input is applied. The corresponding plot described in **Figure 6** shows overshoots and it needs relatively reduced settling time. In this simulation, the poles have 50 Hz of natural frequency and 1 g of absolute gain.

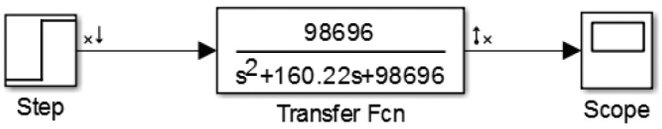

Figure 5. Matlab Simulink diagram (without RC filter).

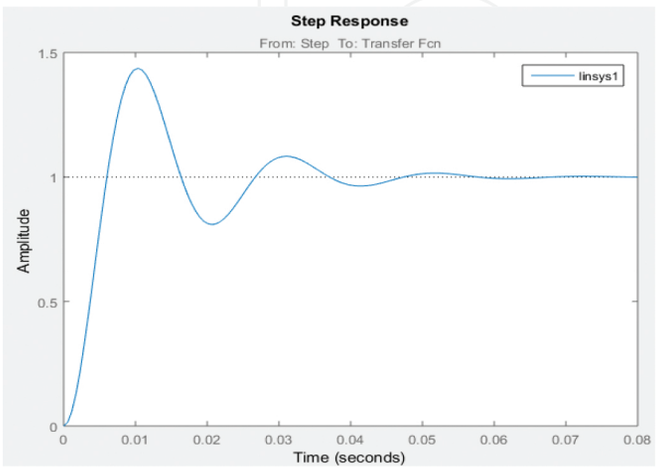

Figure 6. Step response (without RC filter).

http://dx.doi.org/10.5772/66215

Since this transfer function may be affected by the zeros, therefore by adding low pass RC filter to the post amplifier, the stability and accuracy of this circuit would be improved. In this case, the RC filter adds one more pole as summarized in **Table 1**. This proves that the calculated poles are placed in the left half of the *s*-plane as well.

	*P*1	*P*2	*P*3
Real (rad/s)	−222.1	−222.1	−1000
Imaginary (rad/s)	222.1	−222.1	0

Table 1. Pole placement of FBA-23 in 50 Hz and 1 g

The full transfer function of the electrical circuit in 50 Hz has three poles as shown in Eq. (12).

$$TF_{\mathrm{RC}} = \frac{98696}{s^3 + 1160.225s^2 + 258921s + 98696000} \tag{12}$$

Figure 7 shows the Matlab Simulink results when a step input is applied. **Figure 8** also shows almost the same plot disregarding the existence of the RC filter.

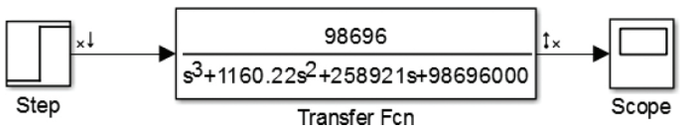

Figure 7. Matlab Simulink diagram (with RC filter).

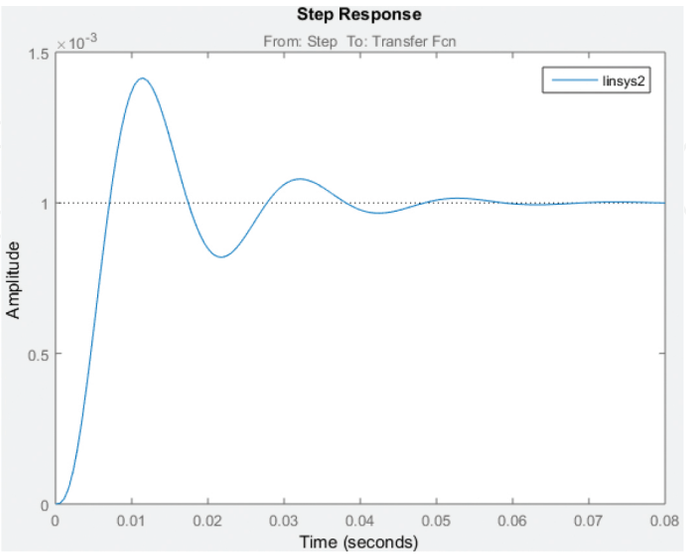

Figure 8. Step response (with RC filter).

3.1.2. Servo acceleration with feedback loop

In this section, the servo acceleration with a feedback loop type accelerometer (AC-23 by Geosig), which consists of geophone and electrical circuits, is discussed. The geophone response can be seen from two viewpoints:

- With a constant velocity, amplitude applied to the geophone.
- With a constant acceleration, amplitude applied to the geophone.

Figure 9 represents the response curve of Geophone at 4.5 Hz.

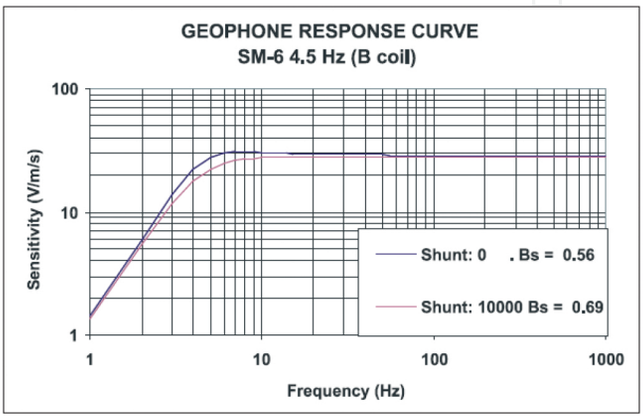

Figure 9. Geophone response curve (4.5Hz) [5].

The relationship between these two points of view is a rotation when plotted with log-log axis scales. In **Figure 10**, the principle of Geophone is drawn. When the motion on the *x*-axis is incident then Geophone generates the open-loop signal which has peak response of 4.5 Hz.

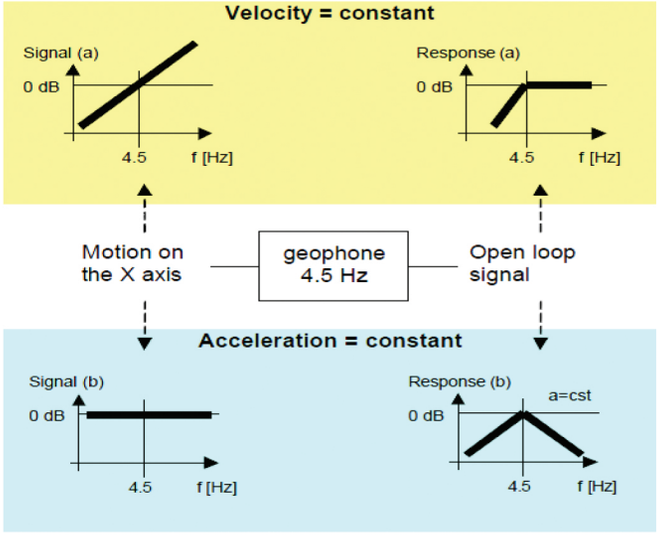

Figure 10. Principle of Geophone [6].

The geophone is a long coil travel version and the extra coil travel offers an advantage for higher tilt requirements where larger amplitude signals may be encountered. A range of natural frequencies is available from 4.5 Hz to 14 Hz, providing a choice of the correct geophone for a wide variety of applications. The geophone is suitable for detecting an extensive range of ground motion.

The AC-23 provides over-damping the geophones with a feedback amplifier in a bridge circuit. The principle of over-damping geophones is done by applying a voltage on the geophone, which has opposite polarity from the voltage, which is induced by the moving geophone coil. Since the voltage induced by the geophone coil is proportional to the velocity, the externally applied voltage is also proportional to it. This results in a current in the coil (~force), which is also proportional to the velocity and therefore is a "damping" current, or additional damping. Increasing this damping further will lead to a resulting output that is proportional to acceleration.

The function of the sensor, seen from a constant acceleration point of view is illustrated in **Figure 11**.

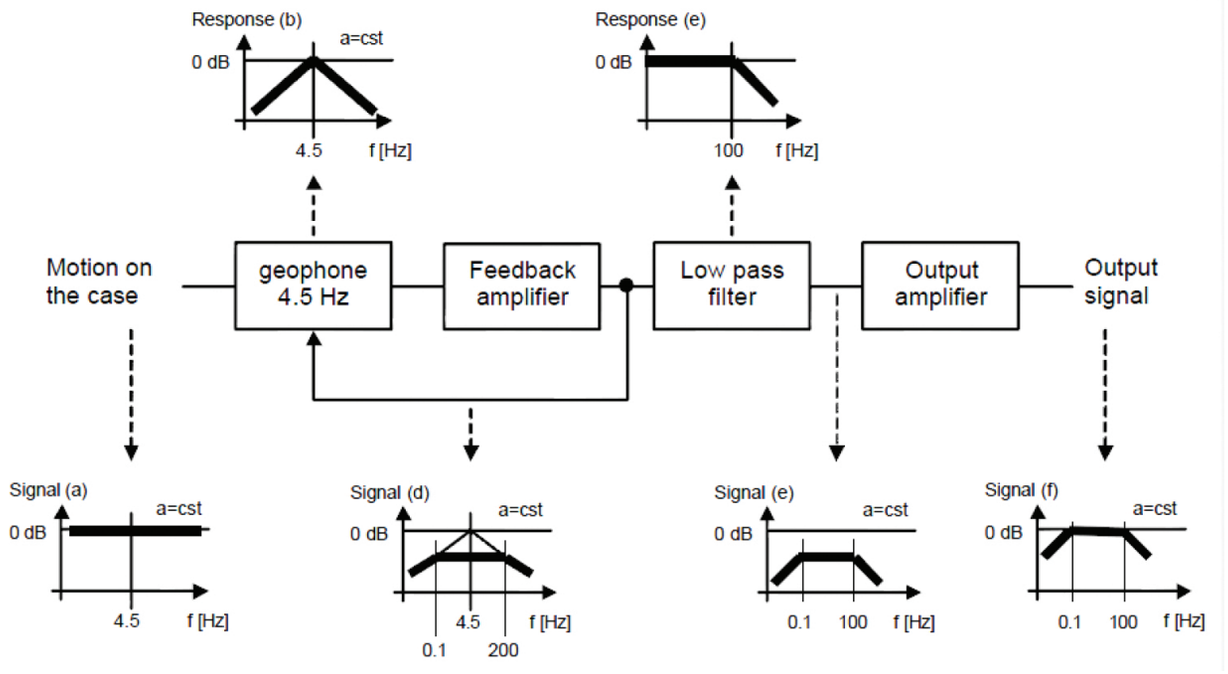

Figure 11. Operational principle of AC-23 [6].

The geophone is connected in a resistor bridge, driven by a feedback amplifier and an inverter, which apply the amplified bridge differential signal in opposite polarity [6]. The amplifier has a fixed gain that will define the bandwidth of the accelerometer. The gain *G* and output *Vo* are represented by Eqs. (13) and (14). **Figure 12** shows the equivalent circuit for the linear servo-balanced accelerometer.

$$G = 1 + \left(\frac{Z_2}{Z_1} \right) \tag{13}$$

$$V_0 = G \cdot V_i = \left(1 + \frac{Z_2}{Z_1} \right) \cdot V_i \tag{14}$$

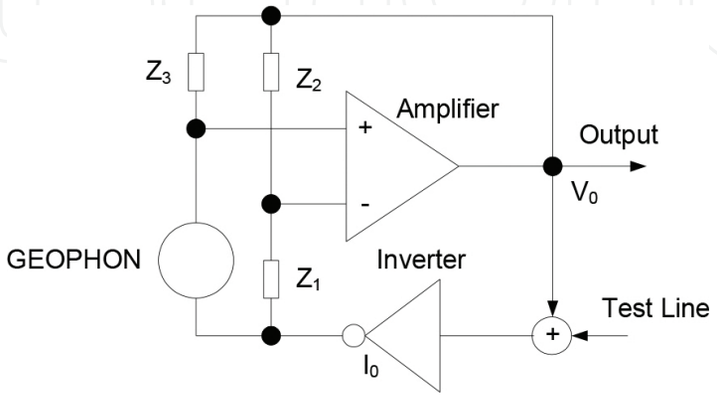

Figure 12. Equivalent circuit for AC-23 (linear servo balanced accelerometer) [6].

In **Figure 12**, the test-line shifts the voltage to one side of the bridge, which produces a current flow in the geophone, resulting in a displacement step of the seismic mass. The movement of the mass generates a voltage across the Geophone, which is detected by the differential amplifier and induces an output signal. The effect of the test signal on the bridge is cancelled by the differential input of the amplifier.

In this part, the Geophone transfer function transfer is analysed in order to define how the sensor generates open-loop transfer function as depicted in Eq. (13).

$$TF = \frac{1.564s}{0.1251s^2 + 1.514s + 1} \tag{15}$$

The transfer function in Eq. (15) has two poles and one zero. In this work, the MATLAB script of Geophone is used to illustrate the response curve under step input condition as shown in **Figure 13**.

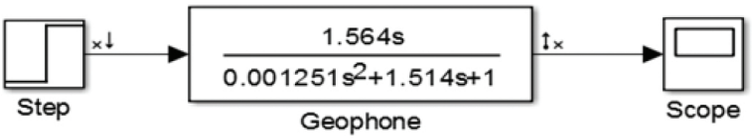

Figure 13. Open-loop transfer function of Geophone.

http://dx.doi.org/10.5772/66215

The transfer function plotted as the frequency range vs. relative response to the acceleration is shown in **Figure 14**.

If a unit step function is applied to the transfer function, the response as in **Figure 15** is obtained.

In this case, the magnitude and the phase can be drawn by the Bode plot as seen in **Figure 16**.

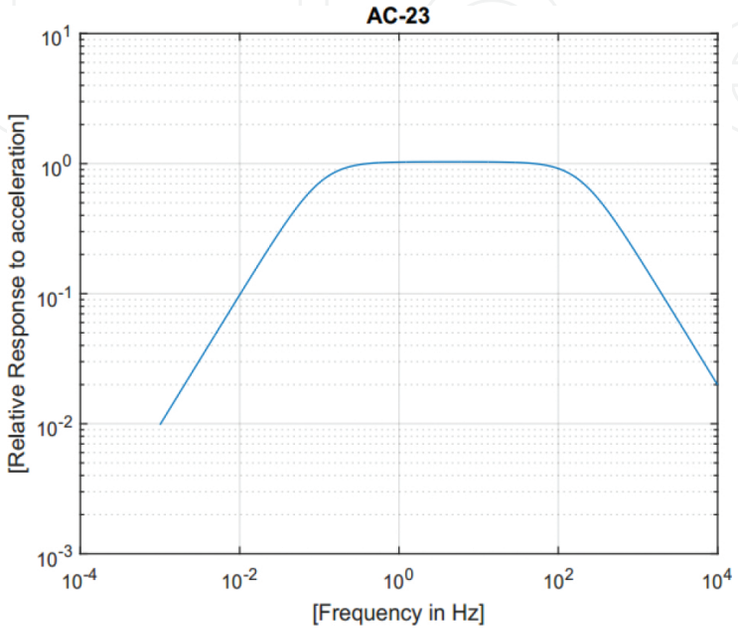

Figure 14. Transfer function plotted by the frequency vs. relative response to the acceleration.

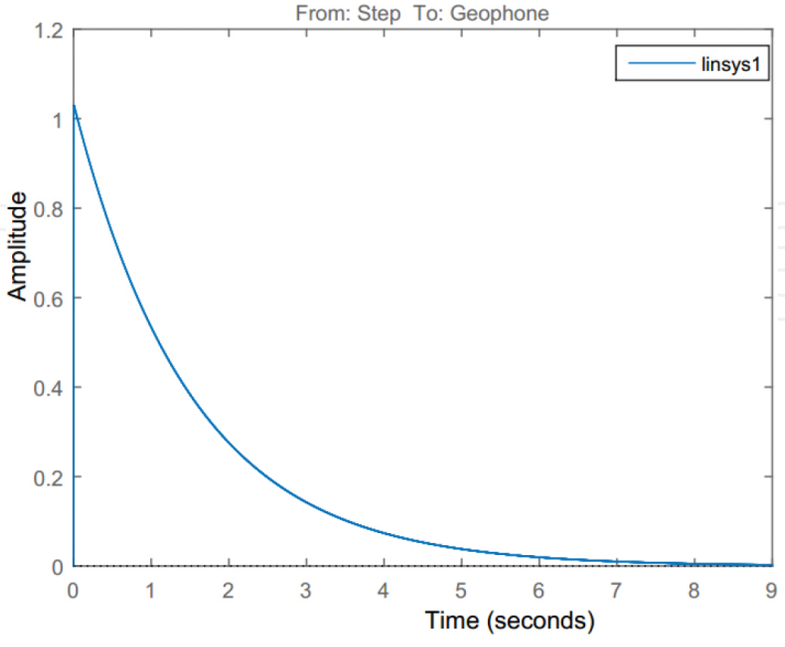

Figure 15. Step response.

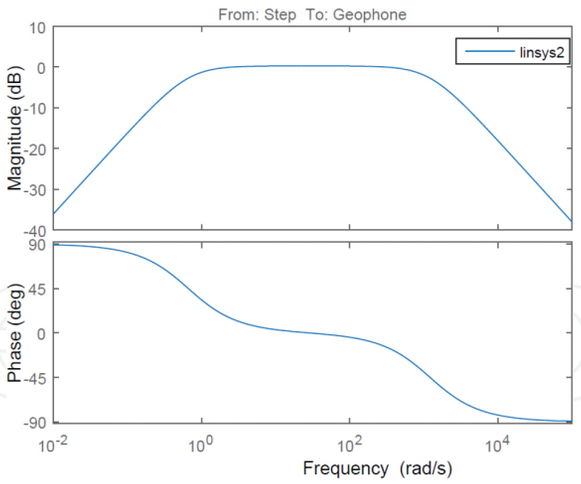

Figure 16. Bode plot.

4. Application of seismic instrument

In this chapter, two application examples for the NPP (nuclear power plant) are discussed with their designs. They are SMS (seismic monitoring system) and ASTS (automatic seismic trip system). SMS detects the seismic wave and provides alarms to the NPP operators. The operator then makes a decision whether or not to trip the nuclear reactor. ASTS has an automatic trip function, if the peak acceleration of the incident wave exceeds, the pre-determined level trigger the reactor trip automatically. In the protection view-point, SMS provides alarms for the manual trip while ASTS provides automatic protection.

4.1. Seismic monitoring system

The SMS consists of tri-axial accelerometers and a seismic monitoring cabinet which is located in an electrical equipment room in unit one (only one unit). The cabinet contains recorders, a playback and analysis unit, an annunciator, a seismic switch, test units and an uninterruptible power supply.

The signal flow from the accelerometer to the seismic monitoring system is shown in **Figure 17**. From the accelerometer, the voltage signal is transmitted to the seismic monitoring cabinet and is converted by electronics into a signal proportional to the acceleration. The acceleration signal can activate recorders and/or local and MCR annunciators/alarms according to its magnitude.

When the acceleration of earthquake exceeds the seismic trigger or set-points for OBE (Operating Basis Earthquake or Event) or SSE (Safe Shutdown Earthquake), the alarm is provided on the local annunciator panel of the seismic monitoring cabinet and that of large panel display system (LDPS) in main control room or alternatively in the remote shutdown room. That event also activates the time-history recorder(s) in the seismic monitoring cabinet.

http://dx.doi.org/10.5772/66215

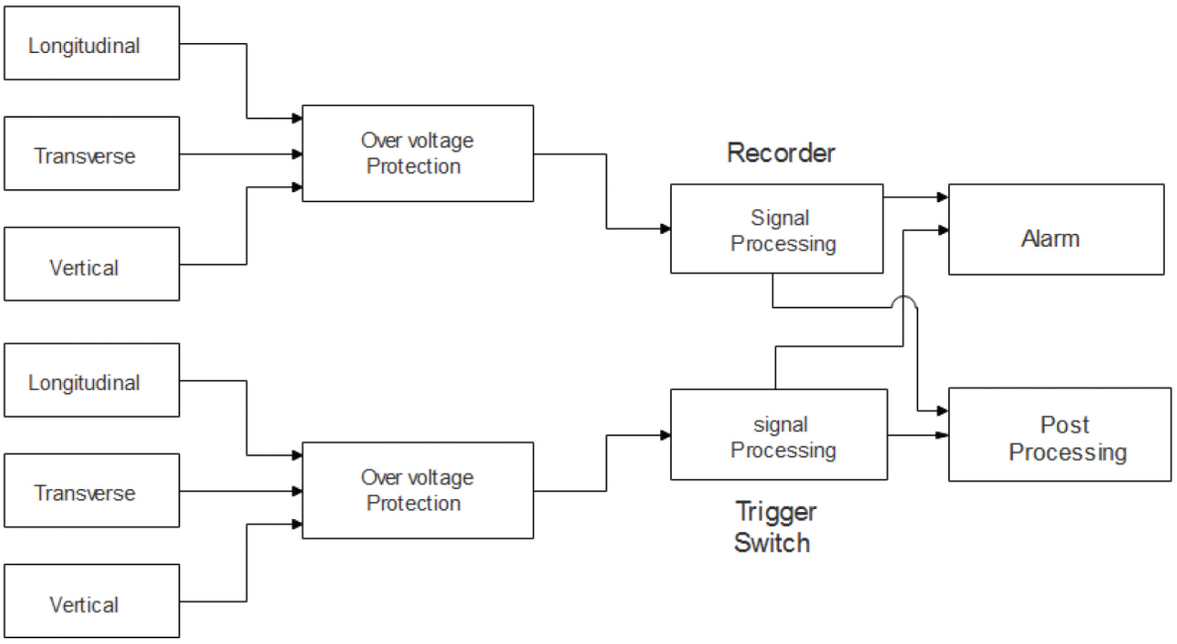

Figure 17. SMS block diagram.

4.2. Automatic seismic trip system

ASTS continuously monitor PGA (peak ground acceleration) from the seismic wave and automatically generates the trip signal. As shown in **Figure 18**, the seismic signal detected by the accelerometer is filtered, rectified and converted to the current. The sensor module is to cut off the frequency ranges over 10 Hz in order to pick out the strong motion of the earthquake. Since the seismic signal has a positive and negative signal, a rectifier circuit is added. The rectifier converts the bipolar signal to the unipolar.

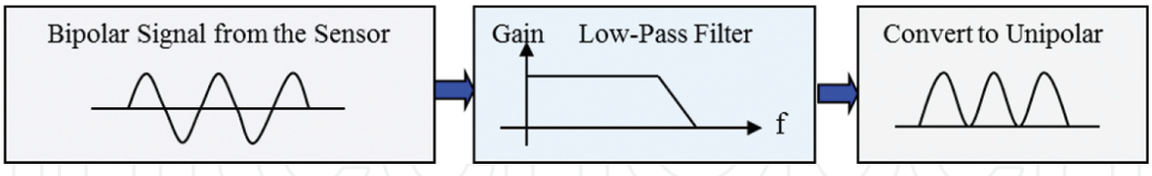

Figure 18. Conceptual diagram of sensor module for signal processing [7].

The overall scheme of ASTS is shown in **Figure 19**. The sensor output is interfaced with digital input card at the ASTS cabinet. Even the decision logic is set as two out of four but the system is composed of two independent channels. They are N1 and N2. For isolation between the channels, the digital input/output card is applied. The dotted line on the ASTS cabinet is the scope of trip logic channel N1 and N2. The ASTS cabinet is implemented by digitalized system such as PLC (programmable logic controller), FPGA (field programmable gate array), or DCS (distribute control system). The bi-stable and decision logic are configured with software inside each channel.

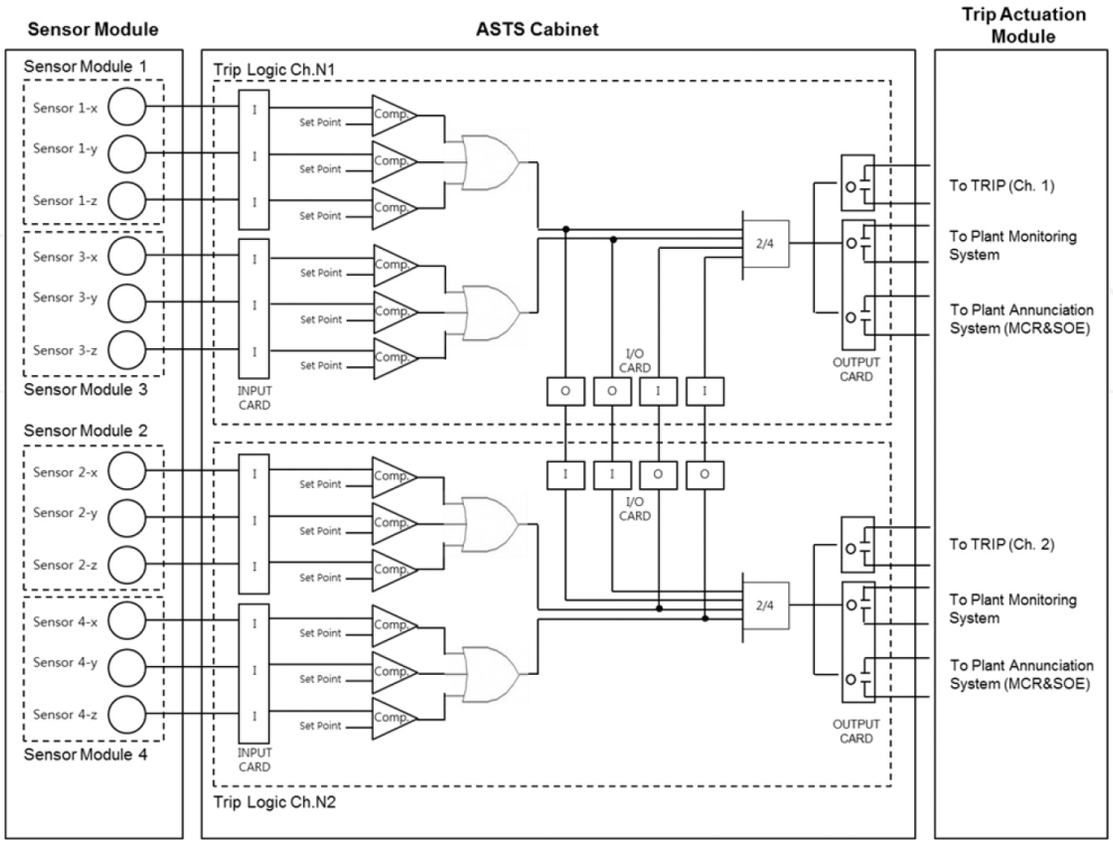

Figure 19. Overall scheme of digitalized ASTS [7].

The operational principles are as follows. When the measured signal exceeds the set-point, the edge triggering happens and the status is set to '0' by comparator actuation. In this case, the latch is engaged due to the edge triggering, and keep the status for 10 s. The purpose of 10-s latch is to synchronize the individual channel for the coincidence logic. If the signals are not properly synchronized, the trip initiation signal may not be actuated during a strong earthquake. ASTS consists of four diverse channel applications. The bi-stable signal from each channel feeds into two-out of-four coincidence logic for generating trip initiation signal.

5. Conclusions

In this work, two measurement principles are analysed to obtain the transfer function plotted by the frequency vs. relative response to the acceleration as well as the step responses. In order to define the sensitivity of open-loop type or closed-loop type with a feedback loop, two sensor types have been used; the force-balanced acceleration and the servo acceleration. The open-loop and closed-loop response when the step input describes the transfer function by plotting it with amplitude and time. The open-loop geophone shows exponentially decreasing function while the force balanced type illustrates overshoot before it is stabilized.

Two application examples for the NPP are discussed with their designs in this work. They are SMS and ASTS. When the Gyeongju earthquake occurred, the main concern in the NPP, whether the peak ground acceleration exceeded in OBE or SSE, was highlighted. The second issue was the frequency range determining the manual or automatic reactor trip. ASTS eliminates frequency over 10 Hz for generating a trip signal. Through Gyeongju earthquake the adequacy of this theory has been proved. The third issue that arose in ASTS design was a latching time of 10 s to synchronize the individual channel for the coincidence logic. This issue needs to be resolved by analysing the seismic waves in Gyeongju.

Author details

Jae Cheon Jung

Address all correspondence to: jcjung@kings.ac.kr

KEPCO International Nuclear Graduate School, Seosang-myeon, Ulju-gun, Ulsan, Republic of Korea

References

[1] "Strongest-ever earthquake hits Korea, tremors felt nationwide". The Korea Times. September 12, 2016. [Accessed 2016. 10].

[2] Katsuhiko Ogata, "Modern Control Engineering", 3rd ed. Chapter 3, New Jersey: Prentice-Hall; 1997. pp. 83–84

[3] Dept. of earth and environmental, Ludwig Maximilians Universiat https://www.geophysik.uni-muenchen.de/.../2_ms_seismic_instruments.pdf [Accessed 2016. 08]

[4] Kinemetrics FBA-23 User Manual, https://nees.org/data/get/facility/sensorModels/180/Documentation/FBA23.pdf [Accessed 2016. 08]

[5] Input/Output, SM-6 Geophone, http://www.iongeo.com/content/documents/.../DS_SEN_121026SM6.pdf [Accessed 2016. 08]

[6] GeoSig, AC-23 User Manual, http://www.geosig.com/files/GS_AC-23_UserManual_V12.pdf [Accessed 2016. 08]

[7] JC. Jung, Design of the Digitalized Automatic Seismic Trip System for Nuclear Power Plants, Nuclear Engineering and Technology, 46(2), 2014, pp. 235–246, http://dx.doi.org/10.5516/NET.04.2013.041;

IntechOpen

IntechOpen